Flight Test Results of ALFLEX Guidance, Navigation and Control System

Hiroyuki ONUMA[*1], Tomoji IWASAKI[*1], Yasuhiro YAMAGUCHI[*1], Keita GOTO[*1], Saori MIZUTANI[*1], Yoshikazu MIYAZAWA[*2], Toshikazu MOTODA[*2], and Tatsushi IZUMI[*3]

ABSTRACT

This paper discusses the flight test results of the guidance, navigation and control (GNC) system developed for the Automatic Landing FLight EXperiment, ALFLEX. The flight tests were successful in every respect, which shows the GNC system is adequate for automatic landing. In this paper, we analyze the flight test data concerning the GNC system, and also discuss the results of designing the GNC system.

1. Introduction

ALFLEX is the experiment vehicle that is being used to develop the automatic landing technology for a future unmanned re-entry space vehicle. The development of ALFLEX Guidance, Navigation and Control system is one of the most important development elements.

The performance of Guidance, Navigation and Control system was demonstrated by the success of the flight experiment at Woomera, Australia. After the flight experiment, we analyzed flight experiment data in detail. This paper reports flight test results concerning ALFLEX Guidance, Navigation and Control system including analyzing the results of flight data. Also, this paper reports the designed results of the ALFLEX Guidance, Navigation and Control system.

2. Evaluation of The Hybrid Navigation Law

The configuration of the navigation system for ALFLEX is shown in Fig. 2-1. FCC is designed to calculate the positions and velocities of the vehicle with the following two Hybrid Navigation Laws, which are switched according to the flight phase of ALFLEX. The switching sequences are shown in Fig. 2-2. And IMU is designed to calculate the attitudes with the inertial navigation algorithm.

(1) IMU-DGPS Hybrid Navigation Law

For the Hanging Flight phase, we have designed DGPS-aided navigation law. The purposes of this navigation law are to calculate the navigation data for leading the vehicle to its releasing area, which are located around the point 2.7km before the runway end and at the height of 1500m, and to give the initial values for IMU-MLS-RA Hybrid Navigation Law which is used in the Free Flight phase.

(2) IMU-MLS-RA Hybrid Navigation Law

For the Free Flight phase, we have designed MLS/RA-aided navigation law, to obtain the navigation data precisely and rapidly for guiding the vehicle on its nominal trajectory, especially after the flare of the vehicle.

In this paragraph, we describe the precision of the Hybrid Navigation Law at representative points on the flight path (comparison with the results measured by Laser Tracker), and the position error transitions in the Free Flight phase.

2.1 The precision at representative points (comparison with the results measured by Laser Tracker)

From the results of 13 flight experiments at Woomera Airfield, the position and velocity errors of the Hybrid Navigation at the following three representative points are shown in Table 2-1.

[*1]Mitsubishi Heavy Industries Co. Ltd., Nagoya Aerospace Systems, Nagoya, Japan
[*2]National Aerospace Laboratory, Tokyo, Japan
[*3]National Space Development Agency of Japan, Tokyo, Japan

This document is provided by JAXA.

- the point at which the Hybrid Navigation Law is switched from IMU-DGPS to IMU-MLS-RA
- the point at which the vehicle is released
- the point at which the vehicle touches down

In these comparisons, the true positions or velocities are calculated with FPR (Flight Path Reconstruction) methods after the flight experiments.

Through all of the flight experiments, the requirements for the Hybrid Navigation Law are satisfied, except for the velocity error of z-axis (altitude) at the point of touch down. This is due to the fluctuation of the altitude data of RA in low altitude, and the high feedback gain of the IMU-RA Hybrid Navigation Filter in order to achieve fast response for the altitude data of RA.

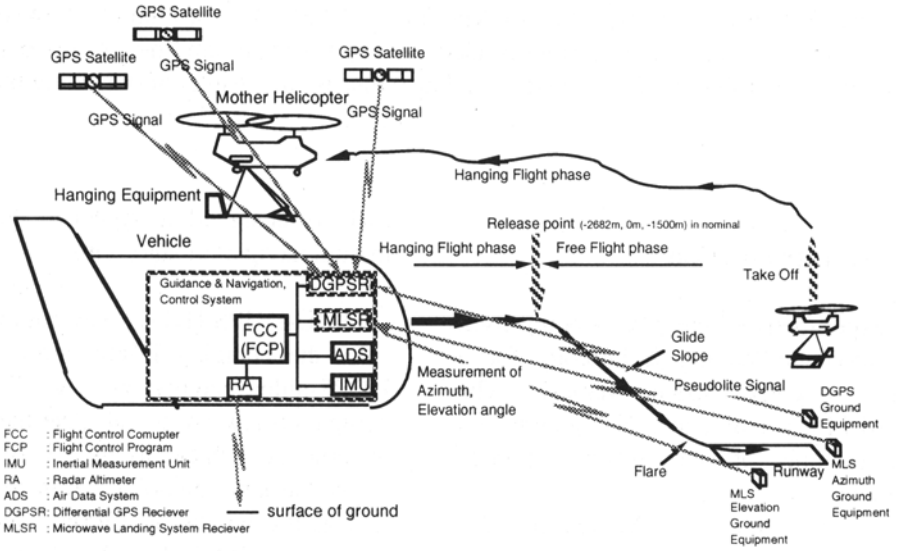

Fig.2-1 ALFLEX Navigation System

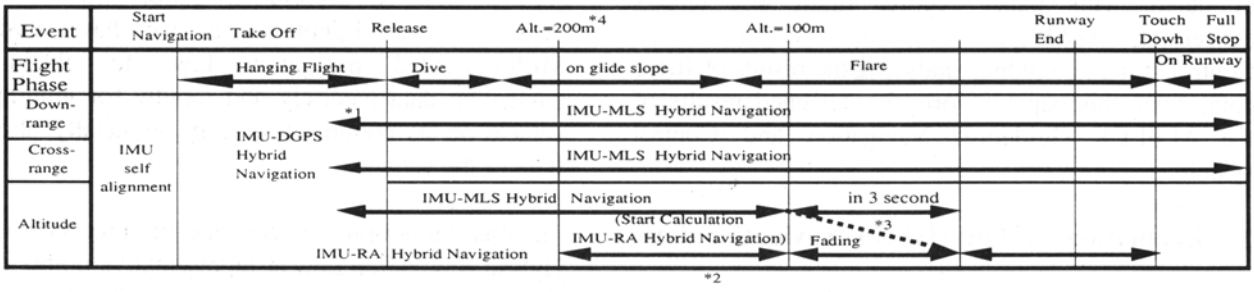

*1) Before releasing the vehicle, start calculation of IMU-MLS Hybrid Navigation with the positions, velocities estimated by IMU-DGPS Hybrid Navigation as the initial value.
*2) Start calculation of IMU-RA Hybrid Navigation, before using as Navigation data.
*3) Fade the navigation data from IMU-MLS Hybrid Navigation to IMU-RA Hybrid Navigation gradually.
*4)Start calculation of IMU-RA Hybrid Navigation at the height of 200m .

Fig.2-2 Sequence of Hybrid Navigation

This document is provided by JAXA.

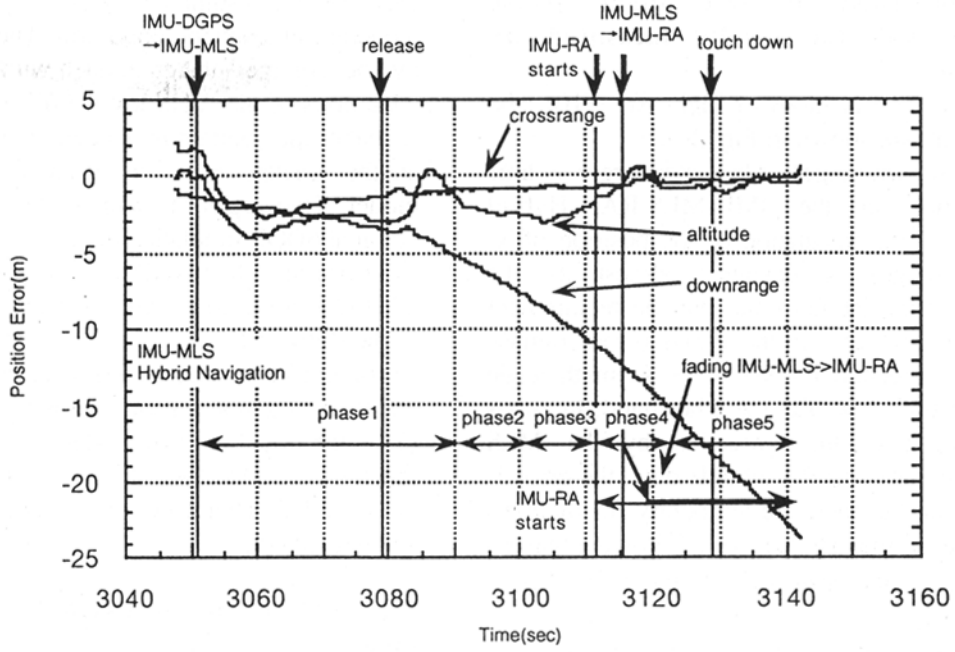

Fig.2-3 Position Error of Hybrid Navigation (Compared with FPR)

Table 2-1 Position Error of Hybrid Navigation (Compared with FPR)

Flight No.	Navigation Error at Starting IMU-MLS-RA						Navigation Error at Release						Navigation Error at Touch Down					
	position(m)			velocity(m/s)			position(m)			velocity(m/s)			position(m)			velocity(m/s)		
	X	Y	Z	X	Y	Z	X	Y	Z	X	Y	Z	X	Y	Z	X	Y	Z
F101	-1.45	1.49	0.01	-0.06	-0.2	-0.21	-3.66	-1.41	2.95	-0.08	0.09	-0.07	-18.79	-0.31	0.77	-0.37	0.04	-0.16
F002	-1.37	1.99	-2.97	-0.05	0.09	-0.07	-2.87	-1.34	2.93	-0.11	0.04	-0.09	-16.84	-0.45	0.07	-0.35	0.1	-0.39
F103	-2.62	6.32	-0.94	0.05	0.15	-0.03	-3.46	-0.61	3.18	-0.05	0.02	-0.08	-16.27	-0.04	-0.7	-0.22	0.02	-0.22
F004	LT is not tracking						14.14	-1.6	-5.74	0.37	0.03	-0.27	28.25	-0.04	-0.11	0.89	0.48	-0.88
F005	2.18	-1.88	-0.31	0.07	-0.06	-0.05	3.05	-0.99	-0.19	0.02	0.07	-0.19	-8.62	-0.11	0.24	-0.13	-0.08	0.19
F006	-1.67	-2.11	-7.24	-0.06	-0.08	-0.16	-3.98	-0.85	3.36	-0.05	0.06	0.09	-19.87	-0.57	0.06	-0.16	0.05	-0.38
F007	-4.15	0.48	-3.07	-0.12	0.01	-0.42	-8.71	-0.96	6.51	-0.22	0.12	0	-27.78	-0.49	0.18	-0.31	0.12	-0.27
F008	-1.25	1.96	-2.84	-0.04	0.04	-0.04	-3.37	-1.28	3.16	-0.03	0.14	0.14	-15.86	-0.45	-0.22	-0.18	-0.06	0.13
F009	-3.16	1.52	-2.9	-0.08	0.06	-0.22	-6.69	-1.41	5.23	-0.12	-0.08	0.12	-26.83	-0.41	0.18	-0.25	0.14	-0.61
F010	-0.37	-1.3	1.69	-0.02	-0.08	-0.18	-1.14	-0.14	2.6	-0.02	0.05	-0.16	-14.62	-0.56	-0.49	-0.16	0.04	-0.29
F011	-3.57	0.7	-2.6	-0.04	-0.06	-0.15	-4.71	-1.34	3.42	-0.12	0	-0.21	-20.41	-0.36	0.33	0.01	0.08	-0.46
F012	-0.66	-0.64	-0.67	0.1	0.07	-0.14	2.64	-1.31	0.58	0.18	0.12	-0.19	0.99	-0.61	0.01	0.53	0	-0.93
F013	0.59	0.44	7.26	0	-0.02	-0.18	1.57	-1.08	1.26	0.13	0.02	-0.14	-0.92	-0.63	0.38	0.61	0.09	-0.86
require-ment	not required						less than 25			less than 0.5			less than 60	less than 8	less than 0.8	less than 2	less than 0.5	less than 0.5

This document is provided by JAXA.

2.2 The precision in free flight phase (comparison with the results measured by Laser Tracker).

The position error transitions of flight No. F101, the first experiment, are shown in Fig. 2-3.

In the x-axis (down range), it becomes larger as time increases, since in the IMU-MLS-RA Hybrid Navigation Law, the calculation of the position of x-axis (down range) is designed almost as the accumulation of the inertial data, but the requirement for this axis is satisfied. In the y-axis (cross range), owing to the correction by the MLS Azimuth angle data, the error stays low. On the other hand, in z-axis (altitude), owing to the correction by the MLS Elevation angle data and RA altitude data, the error is sufficiently small but there are temporary fluctuations. These fluctuations may be due to the following reasons

- the lacking for the correction of the lever-arm of MLS antenna
- the uncertainty of the time delay of MLS data
- the fluctuation of the altitude data of RA in low altitude

2.3 Summary of Evaluating The Hybrid Navigation Law

From the results of 13 flight experiments at Woomera Airfield, we have confirmed the adequacy of the Hybrid Navigation Law for ALFLEX. We have also obtained various data, such as the characteristics of each sensor, which will be useful for the design of the Hybrid Navigation Law for HOPE in the near future.

3. Evaluation of The Guidance Law

ALFLEX has finished 13 automatic landing flight tests successfully. The touch down conditions in all flight tests are shown in Table 3-1. All of the touch down requirements were satisfied.

But the touch down points shifted forward about 150m (maximum 214.4m, minimum 79.8m) beyond the nominal design point. To find the cause of the touch down overshoot, the 6 DOF simulation model which reproduces the flight test results is constructed. This paragraph discusses ALFLEX flight data before touch down, because it is necessary for touch down condition of simulation model to be exactly the same as that of the flight test in order to simulate ALFLEX behavior after touch down.

3.1 6DOF simulation model

Flight test no. F002 is reproduced in this paragraph because this test was conducted for the basic characteristic estimation phase (phase 1) in the moderate atmospheric condition. The simulation result by the nominal design model with the same initial conditions of the flight test (F002) is almost the same as that of the nominal initial condition, so there will be another unexpected error different from the nominal model. Two types of error models are added to the nominal 6DOF simulation model:

(1) Error model derived from the flight data

(2) Error model to get the same touch down condition as the flight test.

Error model (1) mainly consists of the wind model and the navigation sensor error model, and error model (2) is the possible error model to reproduce the same touch down condition of flight test after error model (1) is added. Therefore, error model (2) should be as small as possible.

3.1.1 Error model derived from the flight data

[Wind model]

Wind model is the difference between the inertial velocity of the flight test from FPR[*1)] and the airspeed of the flight test from ADS.[*2)]

[Navigation sensor model]

MLS[*3)] and RA[*4)] error models are constructed except for ADS error model, because ADS error is included in the wind model. The sensor models are set to be the same as the flight test.

<MLS error model>

The Azimuth error model (ΔAz) consists of bias and vibration error which is observed in the hanging flight tests. The elevation error model (ΔEl) is proportional to the rate of elevation change:

$$\Delta Az = \delta Az_0 + K_{Az} \sin(2\pi X / X_{Az})$$
$$\Delta El = K_{El}(dEl/dX) \qquad (3\text{-}1)$$

where

$\delta Az_0 = 0.008$ (deg)

$K_{Az} = 0.0$ (deg) X<-2500m or X>-500m

$= 0.020$ (deg) -2500m≤X≤-500m

$X_{Az} = 62.5$ (m)

$K_{El} = 2.5$ (m).

<RA error model>

The hanging flight tests show RA has the bias error, the error which depends on the height, the random noise, and the spike noise at the end of the runway.

This document is provided by JAXA.

Therefore RA error model consists of 4 types of error models:

$$\Delta RA = \delta RA_0 \quad : \text{bias error}$$
$$+\delta RA\_scl(H) \quad : \text{error dependent on height}$$
$$+\delta RA\_spk(X,H) \quad : \text{spike noise}$$
$$+\delta RA\_rndm(X,H) \quad : \text{random noise} \qquad (3\text{-}2)$$

where

δRA_0 = 0.3 (m)

$\delta RA\_scl(H)$ = -0.02H (m) X<100m

= 0.05H - 7.0 (m)

100≤X<200

$\delta RA\_spk(X,H)$

-1 (m) amplitude spike noise input 4 times/sec at X<-60(m) & 10<H<40(m)

$\delta RA\_rndm(X,H)$

3σ = 0.6 (m) X<-60(m) & 0≤H<100(m)

1.2 (m) X<-60(m) &H≥100(m)

0.3 (m) X≥-60(m).

The navigation sensor error of the flight test and simulation model are shown in Fig. 3-1. Two errors seem almost the same.

<Another model>

Measuerd results of the runway height data, and the mass property are used and shown in Table 3-2.

The floating before touch down is reproduced by the 6DOF simulation model with the error model derived from the flight data. But there are differences between the simulation result and that of the flight test, which are touch down conditions, rudder deflection when lateral guidance starts, and so on. To eliminate these differences, following error models are added.

3.1.2 Error model to get the same touch down condition of flight test

<MLS, IMU[*5)] delay time>

MLS data delay time=100 (msec) : 200 (nominal)

IMU data delay time=25 (msec) : 31.25 (nominal) (3-3)

<Lateral aerodynamic force and moment>

CY, Cn, Cl are fixed at the value of α=8deg when α>8deg.

Rudder effect of lateral force and moment is 1.5 times more than nominal aerodynamic data (3-4)

<ADS_β error model>

β bias = 0.15(deg)

(when Mach increases over 0.230)

= 0.25(deg)

(when Mach decreases under 0.224) (3-5)

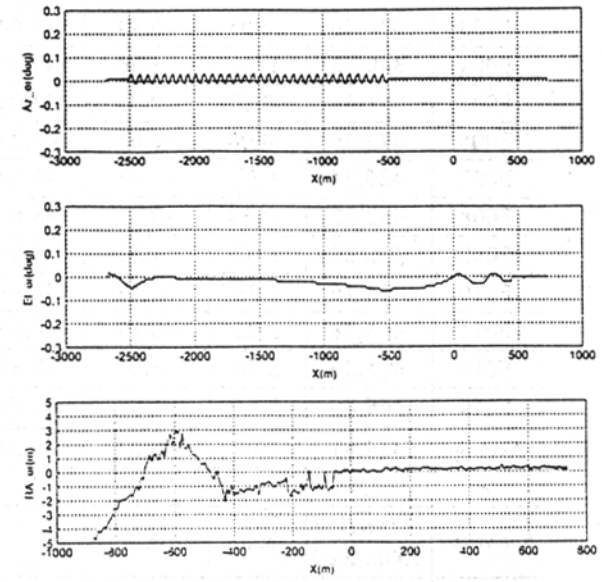

a)F002 Simulation

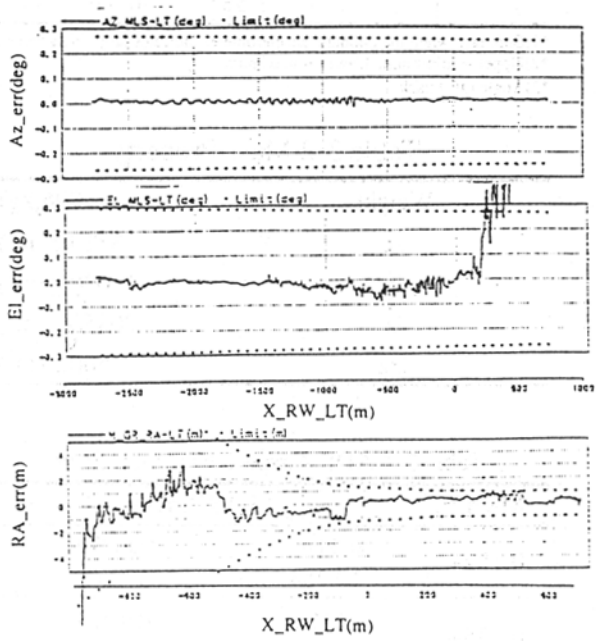

b)F002 Flight Test

Fig. 3-1 Navigation Sensor Error

This document is provided by JAXA.

Table 3-1 Touch Down Condition

T/D condition	T/D point X(m)	Lateral Y(m)	Sink rate*1) dH/dt(m/s)	Airspeed VA(m/s)	Ground speed VG(m/s)	Pitch θ (deg)	Roll ϕ (deg)	Heading ψ (deg)	AOA*3) α (deg)	Side slip β (deg)
Nominal	260.40	-1.00	-0.80	51.90	51.90	11.80	0.30	0.00	13.80	-0.10
F101	420.38	0.40	-1.37	48.08	46.75	13.36	-0.46	0.74	17.09	0.15
F002	451.32	1.60	-0.40	48.63	46.84	13.53	0.46	-0.61	17.49	-0.30
F103	474.78	-0.05	-0.44	48.64	51.50	12.00	-1.25	2.27	16.15	-1.34
F004	340.23	1.76	-1.50	46.71	43.47	8.87	-0.78	-1.42	18.98	1.15
F005	441.11	-3.02	-0.76	47.01	53.63	12.43	-2.11	3.28	16.46	-2.46
F006	474.49	-0.08	-0.65	49.26	52.49	9.71	-0.55	1.39	18.44	0.10
F007	426.58	1.35	-0.43	47.22	50.60	13.23	0.66	-2.09	16.71	0.79
F008	432.22	-1.34	-0.70	48.85	47.78	12.41	-2.13	4.31	15.63	0.26
F009	408.83	3.07	-1.11	48.87	45.57	13.82	0.76	-2.58	16.87	0.36
F010	425.16	2.39	-0.68	48.99	48.91	11.48	0.67	-1.59	15.47	0.47
F011	463.38	3.25	-0.37	48.36	53.37	13.18	0.46	-0.92	16.77	-0.30
F012	423.26	3.56	-1.07	47.82	46.15	13.74	0.92	-3.08	17.36	1.11
F013	366.80	0.55	-1.03	48.56	43.90	13.51	0.15	-0.88	17.72	2.00
Average	426.81	1.03	-0.81	48.23	48.54	12.41	-0.25	-0.09	17.01	0.15
σ	37.44									
Requirement	dispersion 300m(2σ)	±12	≧-3	42~58	≦62	≦23	±10	±8	-	-
Result*2)	149.76	-3.02 3.56	-1.50 -0.37	46.71 49.26	43.47 53.63	8.87 13.82	-2.13 0.92	-3.08 4.31		

*1)Sink rate when the onboard accelerometer indicates large Nz acceleration
*2)Upper = minimum, Lower = maximum
*3)Angle Of Attack

Table 3-2 Mass Property

Weight	796(kg)
Ix	382(kg·m^2)
Iy	1500(kg·m^2)
Iz	2085(kg·m^2)
Ixz	50(kg·m^2)

Table 3-3 Comparison of Touch Down Condition

Data	Simulation	Flight test
Time(sec)	49.8	49.8
X(m)	448.58	451.32
Y(m)	0.64	1.60
dH/dt(m/s)	-0.47	-0.40
Ground speed(m/s)	46.99	46.27
Airspeed(m/s)	48.98	48.63
AOA(deg)	16.90	17.49
Side slip(deg)	-0.7	-0.3
Pitch(deg)	11.73	13.53
Roll(deg)	0.47	0.46
Heading(deg)	0.2	-0.61

Table 3-4 ADS Airspeed Bias Step Error

Mach*1)	ΔEAS*2)(m/s)	
0.182+	-0.5144	AOA≦9
	-1.0288	AOA>9
0.236+	0.2572	AOA≦9
	0.5144	AOA>9
0.224-	-1.5432	8.8≦AOA<12.4
	-2.0576	12.4≦AOA<15
	-2.5720	15≦AOA<17
	0.0000	17≦AOA or AOA<8.8
0.182-	1.0288	

*1)Switching Mach number: "X+" means Mach increases over X,"X-" means Mach decreases under X
*2)Equivalent Airspeed Bias Step Error=EAS(Now)-EAS(Before)

This document is provided by JAXA.

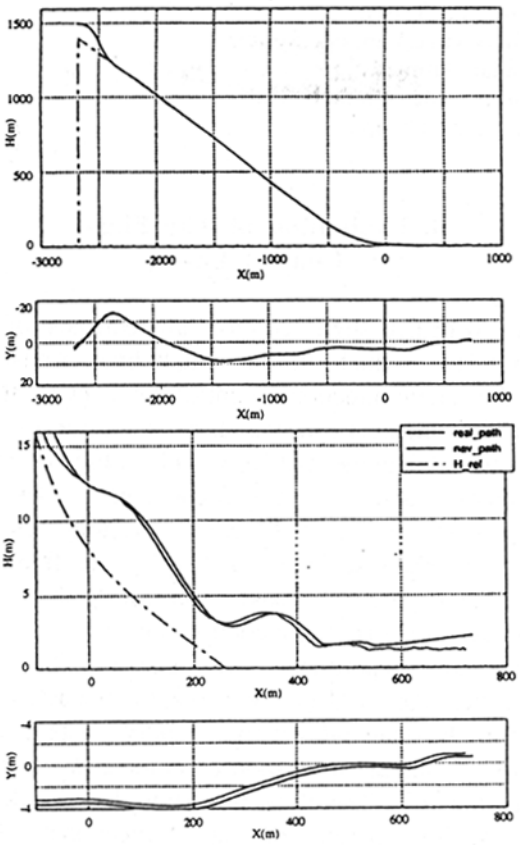

a)Flight Path

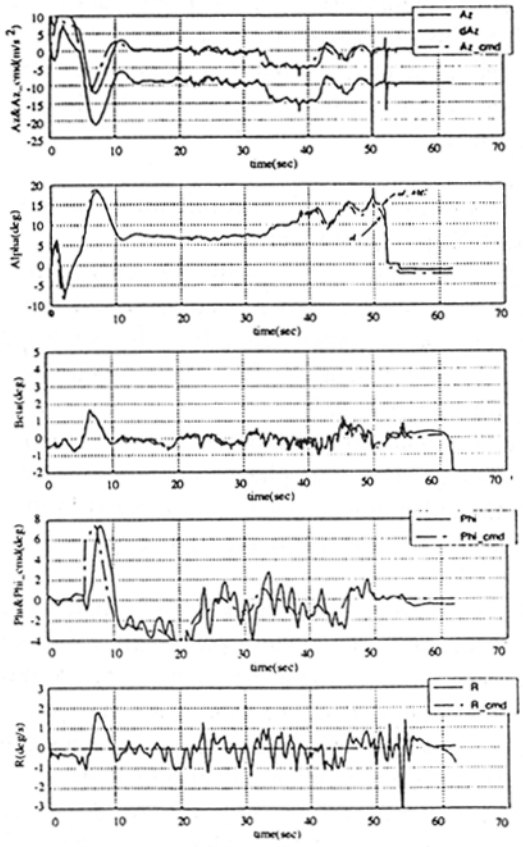

b) Control Value

Fig. 3-2 F002 Simulation Time History

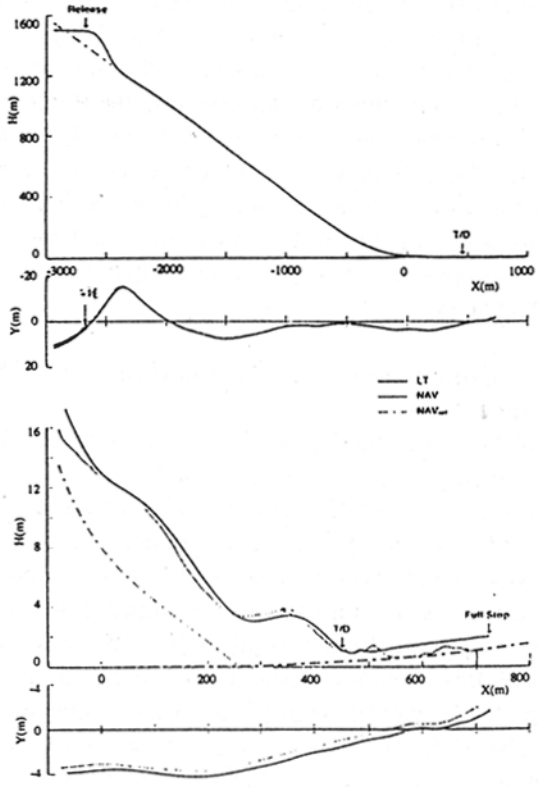

a)Flight Path

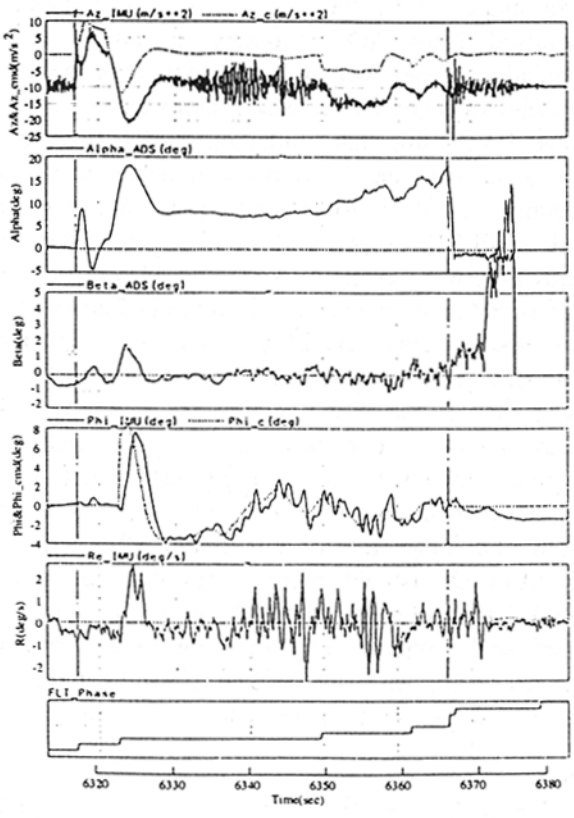

b) Control Value

Fig. 3-3 F002 Flight Test Time History

This document is provided by JAXA.

The simulation result which uses these error models is shown in Fig. 3-2, and that of flight test in Fig. 3-3. And comparison of the touch down condition is shown in Table 3-3. With this simulation model, the flight test touch down condition is reproduced. The (3-4) model decreases the difference of rudder deflection when lateral guidance starts on the steep glide slope, and the (3-5) model eliminates ADS error in the wind model, which is supposed to be negative side slip bias error in this Mach area.

3.2 Conclusion of Evaluation of The Guidance Law

The 6DOF simulation model with the wind model and sensor models of (3-1) to (3-5) is able to reproduce the same result as the F002 flight test. The most effective error model to floating is the wind model, because the simulation result without the wind model shows ALFLEX is not floating and does not touch down over the nominal point. In almost all flight tests, however, the touch down point overshoot was observed, and it is improbable that the wind pattern was similar every time. The ADS data was used to make the wind model, and it is verified that the ADS has a certain error because of ADC*6) software. To investigate the effect of ADS error, instead of the wind model and ADS β error model (3-5), the ADS error model which is supposed from ADC software is added to the simulation model, which is the bias error model of airspeed switched by the Mach number (shown in the Table 3-4). Using that simulation model, floating did not occur with the MLS nominal delay time model (200msec), but the touch down point was over shot and ALFLEX experienced floating when the MLS delay time was 100msec (3-3). The ADS error model means that ADS underestimates the actual airspeed. By this airspeed error ALFLEX flies at the speed faster than that of design, and the energy of ALFLEX is more than at the design condition. A shorter MLS delay time means that the navigation output delay time is smaller than that of the design model, which lessens the energy loss when the navigation output is delayed. Both ADS airspeed error and shorter MLS delay time let ALFLEX fly with more energy than the nominal condition, therefore ALFLEX must fly longer to decrease that energy in the final flare phase. It will be the reason for ALFLEX to float in the final flare and for the excess touch down point.

[Note]
*1)Flight Path Reconstruction: The flight trajectory which is reconstructed from the data of the onboard sensors and the ground support equipment.
*2)Air Data System
*3)Microwave Landing System
*4)Radar Altimeter
*5)Inertial Measurement Unit
*6)Air Data Computer

4. Evaluation of The Flight Control Law

The ALFLEX flight control law consists of two control laws, which are the longitudinal control law and the lateral-directional control law. FCC (Flight Control Computer) executes these two control laws at 80Hz to stabilize the ALFLEX vehicle. Fig. 4-1 shows the block diagram of the flight control law. The performance of the flight control system has been proven to have sufficient ability by the free flight experiment, and we have confirmed the design technique of the H_∞ flight control law.

After the experiment, we analyzed the flight experiment data in detail. We found unexpected flight data in the lateral-directional control system which shows different a response compared with the simulation data. Therefore, in section 4.1, we degrade the stability margin of lateral-directional control system, and tuned the control system to have similar response characteristics as the flight data in order to analyze this phenomenon. In section 4.2, we analyze the lateral-directional control system with the flight vehicle model which is evaluated during the free flight experiment.

4.1 Comparison of Simulation Analysis and Flight Experiment Data

Fig. 4-2 shows step response characteristics of lateral-directional control system obtained from linear analysis. On the other hand, Fig. 4-3 shows the 7th flight experiment data (F007) whose wind disturbance is comparatively small.

Fig. 4-3 indicates that bank-angle response has small vibration at 1Hz. This phenomenon (bank-angle small vibration phenomenon) was not expected in the design and analysis phase before the flight experiment.

We analyzed this bank-angle small vibration phenomenon from the viewpoint of the stability margin decrease, which might be caused by aerodynamic delay (the delay from the time when aileron or rudder move to the time when the vehicle changes direction) or aerodynamic errors of rudder effect, etc.

In the linear analysis of Fig. 4-2, we do not consider the aerodynamic delay. Therefore, the difference

This document is provided by JAXA.

between the simulation and the flight data is caused by the existence of aerodynamic delay. Moreover, it is assumed that aerodynamic error decreases the stability margin of the control system, which causes the difference between the simulation and the flight data.

Then we insert the time-delay-model and the gain-model into the actuator line to decrease the stability margin, and obtain similar response characteristics compared with the flight data.

After tuning the time-delay-model and the gain-model, we obtain the control system with the time-delay-model and gain-model shown in Table 4-1 which has similar characteristics as the flight data. Table 4-2 shows the stability margin of the control system with the model shown in Table 4-1. Fig. 4-4 shows response characteristics, which are obtained from the simulation whose guidance command is given from the flight data (F007), and we can compare the flight data with the simulation result in Fig. 4-4.

From Fig. 4-4, the simulation bank-angle response has similar characteristics as the flight data. However, from Table 4-2, the control system has only a little stability margin, in the aileron loop it has only 0.9dB gain margin and 3.52° phase margin. With this stability margin, the control system may not be able to maintain the stability of the vehicle under strong wind conditions. Moreover, it needs more than 125 ms time-delay-model to obtain similar response characteristics as the flight data, which indicates it is very hard to consider the existence of such a large aerodynamic delay in the control system.

As mentioned above, we estimated the cause of the bank-angle small vibration phenomenon with the time-delay-model and gain-model. As a result, we obtained similar response characteristics as the flight data, but it is very hard to consider this method really simulates real flight control system. Therefore, it is difficult to explain this phenomenon only with the decrease of stability margin. As another cause of this phenomenon, it is assumed the nonlinearity of the actuator system or effects such as side wind. More analysis is needed to explain this phenomenon more clearly.

4.2 Analysis of The ALFLEX Model Error

In the ALFLEX flight experiment, M-sequence control inputs are executed in the control variables to estimate the ALFLEX vehicle model.

As a result, the model estimated by the flight experiment (the "flight model") turned out to have a slight difference from the model that is used in the controller designing process (the "design model"). Therefore, we analyze response characteristics and stability margin with the design model and the flight model.

Fig. 4-5 and Table 4-3 show the step response and stability margin, respectively, of the design model and the flight model at the flight speed of 80m/s. Comparing these step responses, the flight model has a slow response compared with the design model, but the two models have almost the same bank-angle response characteristics when the bank-angle command is given from the guidance function. Bank-angle response characteristics are more important than side-slip response characteristics in the ALFLEX control system because the bank-angle command is used to adjust lateral deviation in the flight. The side-slip angle output of the flight model when the bank-angle command is given is very small, that means cross-decoupling is achieved sufficiently. The stability margin of the flight model is less than that of the design model, but the differences are sufficiently small. Moreover, the gain margin and the time-delay margin that is calculated from the phase margin of the flight model have more than 6dB and about 100ms delay, respectively, which means the flight model system has a sufficient stability margin.

Regarding the bank-angle small vibration phenomenon, it is difficult to explain the phenomenon only with this model error because the step response of the flight model has no vibrant characteristics.

4.3 Summary of Evaluating The Control Law

Although there is a slight difference between the simulation and flight data, the control system of ALFLEX was verified to have sufficient landing performance, desirable response characteristics, and stabilizing ability for the vehicle under wind disturbances in the 13 flight experiments. Moreover, in this paragraph, we analyzed the control system with the flight model, and we confirmed the robustness of the control system against deviation of the vehicle model.

The development of the designing flight control system for the space vehicle will be one of the most important design items to realize an adequate stability margin against the uncertainty which is inherent in the design process.

This document is provided by JAXA.

Table 4-1 Gain and delay inserted model

	aileron loop	rudder loop
(inserted) gain model	1.25	0.95
(inserted) delay model	125ms	100ms

Table 4-2 Stability margins of the gain and delay inserted model

	aileron loop	rudder loop
gain margin (Frequency)	0.90 dB (at 5.25 rad/s)	1.07 dB (at 4.96 rad/s)
phase margin (Frequency)	3.52 deg (at 4.86 rad/s)	12.2 deg (at 7.10 rad/s)

Table 4-3 Stability margins of design and flight models

		aileron loop	rudder loop
design model	gain margin (Frequency)	8.44 dB (at 10.9 rad/s)	7.69 dB (at 21.0 rad/s)
	phase margin (Frequency)	39.9 deg (at 4.49 rad/s)	56.0 deg (at 7.16 rad/s)
flight model	gain margin (Frequency)	7.05 dB (at 10.1 rad/s)	7.67 dB (at 20.3 rad/s)
	phase margin (Frequency)	29.3 deg (at 4.77 rad/s)	44.1 deg (at 7.79 rad/s)

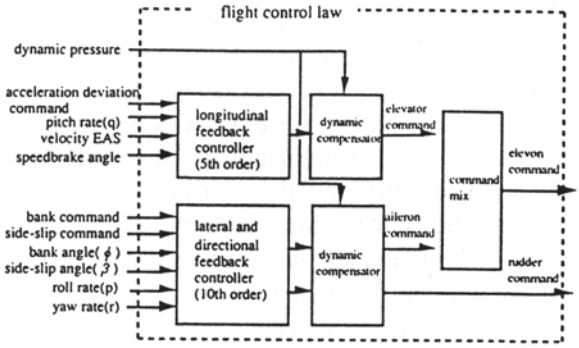

Fig.4-1 Flight Control Law

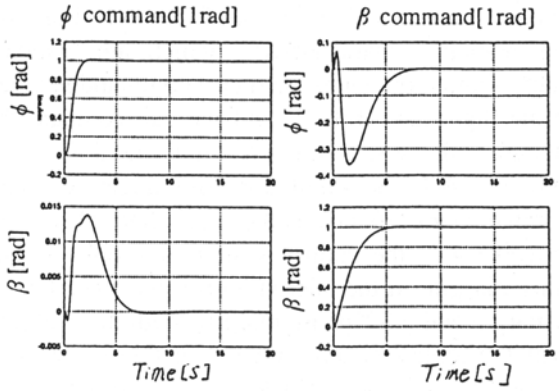

Fig.4-2 Lateral and Directional step response

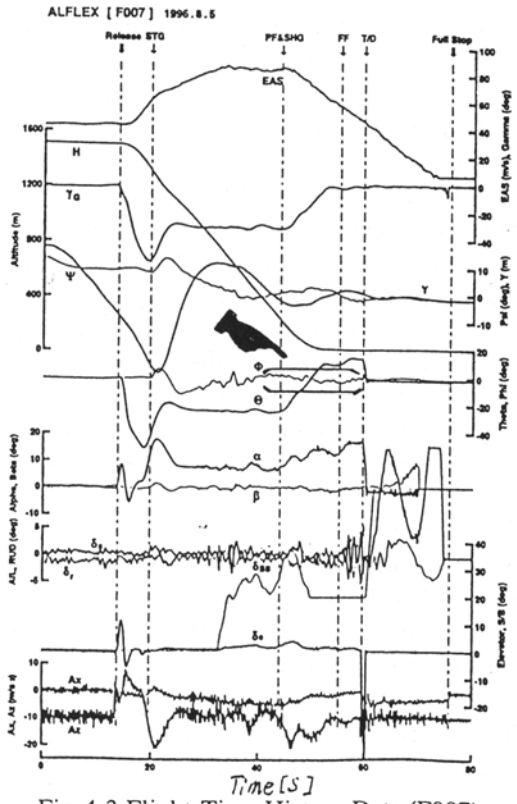

Fig.4-3 Flight Time History Data (F007)

This document is provided by JAXA.

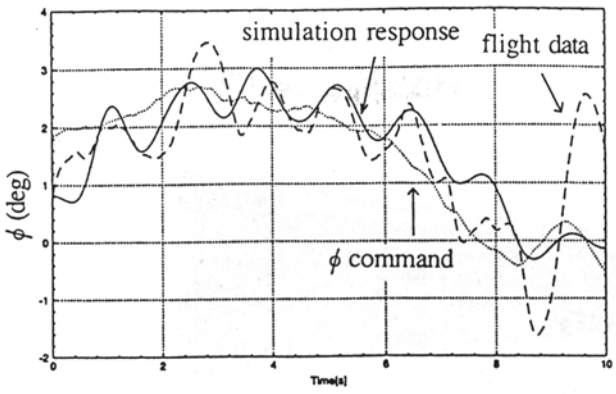

Fig. 4-4 Lateral and Directional response
(bank-angle command from flight data)

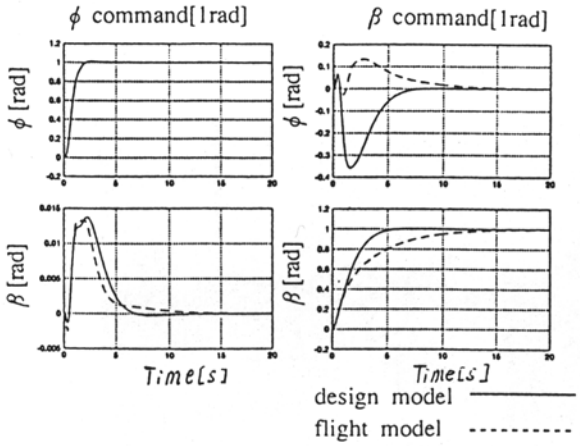

Fig. 4-5 Lateral and Directional step response
(design model and flight model)

5. Summary

We reported on the design results and the analysis result of the flight data concerning the Guidance, Navigation and Control system. It is very important for HOPE development to utilize the results which are obtained during the development of ALFLEX GNC system.

This document is provided by JAXA.

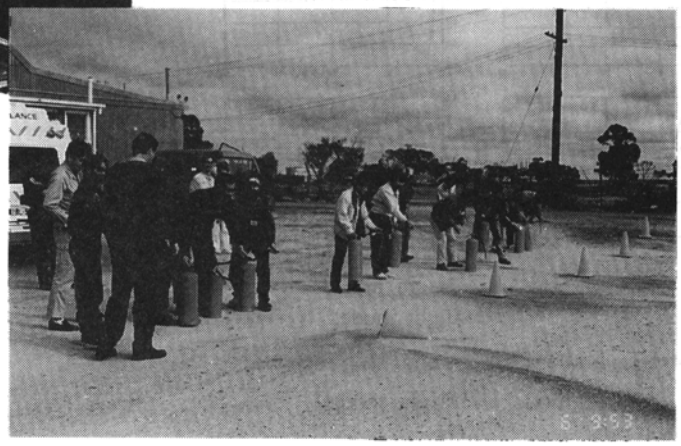

This document is provided by JAXA.